Journal of Applied Mechanics and Technical Physics, Vol. 39, No. 1, 1998

INTERACTION OF A TOLLMIEN–SCHLICHTING WAVE WITH A LOCAL FLOW INHOMOGENEITY

M. V. Ustinov

UDC 532.517

The method of parabolic stability equations is used to study the laminar–turbulent transition in a boundary layer with a stationary velocity inhomogeneity concentrated in a narrow stream. The location of the transition is found as a function of the magnitude and sign of the velocity defect. It is shown that if the inhomogeneity amplitude is small, it affects only the final nonlinear stage of disturbance development. In this case, the location of the transition is independent of the sign of the velocity defect. Having a moderate amplitude, a lower-velocity inhomogeneity shifts the transition location significantly more strongly than a higher-velocity inhomogeneity of similar shape and amplitude. This is caused by amplification of unstable disturbances in the low-velocity region and, conversely, their attenuation in the high-velocity stream. The effect of disturbance amplification in the low-velocity region is shown not to be connected with inflection-type instability. Another explanation of this phenomenon is offered.

It has been found that stationary disturbances in the form of individual or periodic streams with higher or lower flow velocity play an important role in the process of laminar–turbulent transition. These disturbances penetrate into the boundary layer from the external flow or arise because of surface roughness. Butler showed [1] that they can be amplified according to an algebraic law and reach a substantial amplitude. A steady flow inhomogeneity itself, however, does not lead to the transition, but only creates conditions for faster growth of unsteady disturbances whose amplification turbulizes the flow. Thus, study of possible mechanisms of flow instability with a localized or periodic velocity inhomogeneity is an important problem [2–5].

Yu [2] and Fisher [3] studied theoretically the stability of a boundary layer with periodic longitudinal vortices and they identified two types of instability modes. The modes of the first type are similar to Tollmien–Schlichting waves and have the largest growth rates when the inhomogeneity has a small amplitude. A large amplitude of the inhomogeneity gives rise to rapidly growing modes of the second type, which have a high frequency and are related to inviscid instability. Experiments of Kachanov [4] and Bakchinov [5] support the theoretical conclusions of Yu, Fisher, and others [2, 3].

In contrast to [2–5], transversely localized inhomogeneities rather than periodic ones are observed under experimental conditions with an elevated level of free-stream turbulence. The problem of interaction of an instability wave with such an inhomogeneity is solved in the present paper by the method of parabolic stability equations, both the linear and nonlinear evolution of disturbances being studied.

1. Formulation of the Problem. We consider a viscous incompressible flow past a flat plate. The kinematic viscosity of the liquid is ν. At a large distance from the leading edge (to satisfy the boundary-layer approximation) there is a local region of the plate surface through which the liquid is injected or sucked. A stream with higher or lower flow velocity in the boundary layer is formed beyond this region. We study the stability of such a flow at a large distance downstream from the injection (or suction) region. We assume that, as in the boundary layer on a flat plate, unstable disturbances in this flow are periodic in time and almost periodic in the stream direction. We suppose also that the disturbance evolution is quite accurately described

Central Aerohydrodynamic Institute, Zhukovskii 140160. Translated from Prikladnaya Mekhanika i Tekhnicheskaya Fizika, Vol. 39, No. 1, pp. 75–83, January–February, 1998. Original article submitted March 28, 1996; revision submitted June 17, 1996.

0021-8944/98/3901-0065 $20.00

by parabolic equations [6], and specification of the initial conditions at a certain distance L from the leading edge is sufficient to find the solution downstream.

To describe the flow, we introduce a Cartesian coordinate system with the origin at the leading edge of the plate and x, y, z axes directed downstream, parallel to the leading edge and normal to the plate surface, respectively. The scales for coordinates and velocity are the thickness of the boundary layer at the site where the initial conditions are specified $\delta = \sqrt{\nu L/u_\infty}$ and the free-stream velocity u_∞. In these length units, the site of specifying the initial conditions has the dimensionless coordinate $x = \sqrt{u_\infty L/\nu} = R$. To specify the initial conditions for the stationary flow inhomogeneity, we consider the problem of liquid flow in the injection (or suction) region and confine ourselves to the linear problem for low-velocity injection (or suction). To create a solitary stream with higher or lower velocity, the injection (or suction) should be concentrated in a region bounded in y. However, the method of parabolic stability equations that we use below requires periodic initial conditions which can be expanded in a Fourier series with respect to y. Since the problem is linear, the injection (or suction) distribution should also have the form of a Fourier series. Thus, the shape of the injection (or suction) distribution is described by the function

$$g(y) = (1-q)\sum_{n=1}^{N} q^{n-1}\cos n\beta y.$$

For q slightly smaller than unity and for a rather large number of harmonics N, this function is comparatively small [about $(1-q)/2$] on most of a period and has a narrow maximum of the order of unity in the vicinity of $y = 0$. The width of this maximum $\tau = \sqrt{2(1-q)}/\pi\beta$ is small in comparison with the period $T = 2\pi/\beta$. For this type of distribution, each injection or suction zone located in the region of maxima with $y = 0$, $\pm\pi/\beta$, $\pm 2\pi/\beta$, etc. does not affect the neighboring zone and thus generates an isolated velocity inhomogeneity. As the injection or suction distribution relative to x, we use a Gaussian function, i.e., we give a vertical-velocity distribution on the plate surface of the form

$$w(x, y, 0) = \varepsilon \exp\left(-\frac{(x-x_0)^2}{\Delta^2}\right) g(y). \tag{1.1}$$

Here $\varepsilon \ll 1$ is the amplitude, and x_0 and Δ are the position of the center of the injection (or suction) region and its characteristic width, respectively. For simplicity, the boundary-layer flow near the injection (or suction) region is assumed to be plane-parallel with a velocity profile $U_0(z)$ that corresponds to the point of specification of the initial conditions. The steady velocity perturbations $\varepsilon \mathbf{V}_{p0}$ generated by injection or suction are then determined by the Fourier transform method [7] and have the form

$$\begin{gathered}\mathbf{V}_{p0} = \{u_{p0}, v_{p0}, w_{p0}\} = \sum_{n=1}^{N} \mathbf{V}_{0n}, \quad \mathbf{V}_{0n} = \{u_{0n}\cos n\beta y, v_{0n}\sin n\beta y, w_{0n}\cos n\beta y\}, \\ \begin{Bmatrix} u_{0n} \\ v_{0n} \\ w_{0n} \end{Bmatrix}(x, z) = (1-q)q^{n-1}\int_{-\infty}^{+\infty} F(k) \begin{Bmatrix} \hat{u}_n \\ \hat{v}_n \\ \hat{w}_n \end{Bmatrix}(k, z)\, e^{ik(x-x_0)}dk,\end{gathered} \tag{1.2}$$

where $F(k) = (\Delta/\sqrt{4\pi})\exp(-\Delta^2 k^2/4)$ is the Fourier transform of a Gaussian function; $\hat{u}_n$, $\hat{v}_n$, and $\hat{w}_n$ are found by solving the boundary-value problem

$$\begin{gathered}ikU_0(\hat{w}_n'' - \gamma^2\hat{w}_n) - ikU_0''\hat{w}_n = \frac{1}{R}(\hat{w}_n^{IV} - 2\gamma^2\hat{w}_n'' + \gamma^4\hat{w}_n), \\ ikU_0\hat{\eta} - n\beta U_0'\hat{w}_n = \frac{1}{R}(\hat{\eta}'' - \gamma^2\hat{\eta}), \\ \hat{w}_n(0) = 1, \quad \hat{w}_n'(0) = \hat{w}_n(\infty) = \hat{w}_n'(\infty) = \hat{\eta}(0) = \hat{\eta}(\infty) = 0, \quad \gamma^2 = k^2 + (n\beta)^2\end{gathered} \tag{1.3}$$

using the formulas

$$\hat{u}_n = (ik\hat{w}_n' - n\beta\hat{\eta})/\gamma^2, \quad \hat{v}_n = (ik\hat{\eta} - n\beta\hat{w}_n')/\gamma^2.$$

Hereinafter, a prime denotes a derivative with respect to z. The solution of (1.2) for $x = R$ obtained for an injection or suction region located a distance of several characteristic lengths Δ upstream of the initial cross section will be used as the initial conditions for steady velocity perturbations. The initial conditions for time-periodic unstable disturbances are specified as a plane instability wave in the Blasius plane-parallel boundary layer. Thus, the velocity field in the vicinity of the initial cross section is given in the form

$$\mathbf{V}(x,y,z) = \mathbf{V}_0 + \sum_{n=1}^{N} \mathbf{V}_{0n} + \mathbf{V}_{10}(z)\,\mathrm{e}^{\mathrm{i}(\alpha x - \omega t)}, \tag{1.4}$$

where $\mathbf{V}_0 = \{U_0(z), 0, W_0(z)\}$ corresponds to the Blasius boundary layer, $\mathbf{V}_{0n}$ is found from (1.2), and $\mathbf{V}_{10}(z)$ is the profile of velocity fluctuations in the Tollmien–Schlichting wave.

2. Numerical Method. To describe the flow evolution and unstable disturbances, we use the method of parabolic stability equations presented in detail in [6]. As in [6], we represent the velocity field as a superposition of the Blasius boundary-layer flow $\mathbf{V}_0$ and the not necessarily small perturbations $\mathbf{V}_p$:

$$\mathbf{V} = \mathbf{V}_0(x,z) + \mathbf{V}_p(x,y,z,t). \tag{2.1}$$

We assume the velocity perturbations to be periodic with respect to y and t and write them in the form

$$\begin{gathered} \mathbf{V}_p = \sum_{n=0}^{N} \sum_{m=0}^{M} \Big(\mathbf{V}_{mn}(x,z)\,\mathrm{e}^{\mathrm{i}m(\alpha(x)-\omega t)} + \text{c.c.} \Big), \\ \mathbf{V}_{mn} = \{u_{mn}(x,z)\cos n\beta y, v_{mn}(x,z)\sin n\beta y, w_{mn}(x,z)\cos n\beta y\}. \end{gathered} \tag{2.2}$$

The amplitudes $\mathbf{V}_{mn}$ and the wave number α are assumed to be slowly varying functions of x. The characteristic scale on which $\mathbf{V}_{mn}$ and α vary by their magnitude is of the order of R.

To obtain equations for the velocity amplitudes $\mathbf{V}_{mn}$, relations (2.1) and (2.2) and a similar relationship for pressure are substituted into the Navier–Stokes equations. The resultant system is parabolized by eliminating the pressure and omitting terms of the order of $1/R^2$, among which there are terms containing the second derivatives of the amplitudes and the wave number with respect to x. As a result, the problem reduces to the following system of parabolic equations for the amplitudes of individual harmonics:

$$\begin{gathered} \hat{L}^0_{mn} \frac{\partial \mathbf{V}_{mn}}{\partial x} + \hat{L}^1_{mn} \mathbf{V}_{mn} + \frac{d\alpha}{dx} \hat{L}^2_{mn} \mathbf{V}_{mn} = N_{mn}(\mathbf{V}_p), \\ \mathbf{V}_{mn}(0) = \mathbf{V}_{mn}(\infty) = 0, \quad m = 0,\ldots,M; \quad n = 0,\ldots,N. \end{gathered} \tag{2.3}$$

Here $\hat{L}^0_{mn}$, $\hat{L}^1_{mn}$, and $\hat{L}^2_{mn}$ are linear differential operators that include only derivatives with respect to z; the right-hand sides N_{mn} contain nonlinear terms that take into account the contribution of the remaining harmonics. The expressions for the operators $\hat{L}^0_{mn}$, $\hat{L}^1_{mn}$, and $\hat{L}^2_{mn}$ for two-dimensional disturbances are given in [6], and those for three-dimensional disturbances can be found in [8].

The initial conditions for the harmonic amplitudes $\mathbf{V}_{0n}$ $(n = 1,\ldots,N)$ and $\mathbf{V}_{10}$, which determine the steady inhomogeneity and the plane instability wave, were discussed in Sec. 1, and the initial amplitudes of the remaining harmonics were set equal to zero.

Equations (2.3) were solved numerically by the marching method. An implicit second-order scheme with iterations was used for approximation of (2.3) with respect to x. The wave number α versus x was found in the course of solution from the condition of the slowest variation of the arguments of the harmonic amplitudes. Discretization of (2.3) with respect to z was performed using the method of collocations. As the basis functions we used $F_l = z\exp(-z/2)L^{(0)}_l(z)$, $l = 0,1,\ldots,Q-1$, where $L^{(0)}_l(z)$ are the Laguerre polynomials. The zero values of the polynomial $L^{(0)}_Q(z)$ were assumed to be collocation nodes. The number of nodes Q in all calculations was 41. In addition, the method of collocations described was used to solve the boundary-value problem (1.3) and the eigenvalue problem for the Orr–Sommerfeld equation, which are needed to specify the initial conditions for (2.3).

3. Calculation Results. We choose $x = R = 800$ as the initial cross section and confine ourselves to consideration of the interaction between a Tollmien–Schlichting wave with frequency $\omega = 0.032$ and amplitude

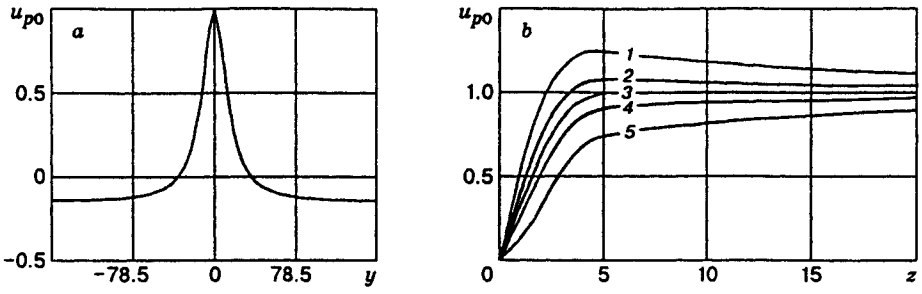

Fig. 1

$a_{10}(R) = 2\max_z |u_{10}(R,z)| = 0.001$ and a steady inhomogeneity of the same shape but different intensity. For this purpose, we choose the following fixed parameters determining the injection (or suction) distribution: $\beta = 0.02$, $q = 0.95$, $\Delta = 20$, $x_0 = 600$, and $N = 41$. The injection intensity ε is varied.

The field of the steady velocity component in the initial cross section is shown in Fig. 1. The transverse distribution of the defect of the longitudinal velocity component u_{p0} for $z = 2.64$, where it reaches the maximum with respect to z, is presented in Fig. 1a (one period is plotted). To obtain a universal curve, the velocity defect is referred to its maximum at $y = 0$. Figure 1b shows velocity profiles for $y = 0$ that were obtained for various injection intensities: $\varepsilon = -1.875\cdot10^{-3}$, $-6.25\cdot10^{-4}$, 0, $6.25\cdot10^{-4}$, and $1.875\cdot10^{-3}$ (curves 1–5). For these values of ε, the maximum velocity defect at the point $y = 0$, $z = 2.64$ amounts to 0.3, 0.1, 0, -0.1, and -0.3, respectively. The last two profiles with negative defects are inflected.

It is seen from Fig. 1 that, for the chosen injection distribution, a narrow region with a noticeable velocity defect and small velocity perturbations in the remaining part of the period is formed. The width of this region $\Delta y \approx 40$ was intentionally selected roughly equal to the characteristic width of the streams with higher and lower velocities that are formed in a boundary layer with a high level of free-stream turbulence [9].

All the results of this study were obtained for the number of harmonics $M = 5$ and $N = 40$ in the velocity equation (2.2). The number of harmonics N in the transverse direction is chosen under the assumption that it is possible to describe the growth of secondary disturbances at the nonlinear stage of transition. Furthermore, the minimum allowable transverse period of disturbances $\alpha \sim 2\pi/N\beta \sim 8$ is approximately one-fifth the width Δy of the inhomogeneity region, which allows us to describe quite accurately the details of the distribution of pulsations with respect to y. The number of harmonics in the direction x is chosen as large as possible for computations on the available computer. A comparison of the results for $M = 2$ and 5 shows a noticeable quantitative disagreement only within the short final stage of disturbance evolution.

To study the influence of a localized flow inhomogeneity of various intensities on the development of unstable disturbances, we calculated the flow evolution for injection intensities corresponding to the maximum velocity defects in the initial cross section $\Delta u_{0m} = \pm0.01$, ±0.1, ±0.2, and ±0.3. Since the method of parabolic stability equations does not yield an adequate description of the late stages of transition, when flow stochastization begins, the computations were terminated after the amplitude of velocity pulsations reached 0.1 at some point of the plane y, z. The point x_* at which this amplitude was attained was assumed to be the position of the laminar–turbulent transition. Hereinafter, the pulsation amplitude is understood as the quantity

$$a(x,y,z) = 2\sqrt{\sum_{m=1}^{M}\left|\sum_{n=0}^{N} u_{mn}(x,z)\cos n\beta y\right|^2},$$

which is $\sqrt{2}$ times larger than the root-mean-square value of velocity pulsations, which is usually measured in experiments.

The dependences of the pulsation amplitudes on x that were obtained for negative and positive velocity defects are shown in Figs. 2 and 3. These and all subsequent pulsation amplitudes correspond to a constant distance from the wall $z_0 = 2.64$, at which the velocity defect is maximum with respect to z. The dashed

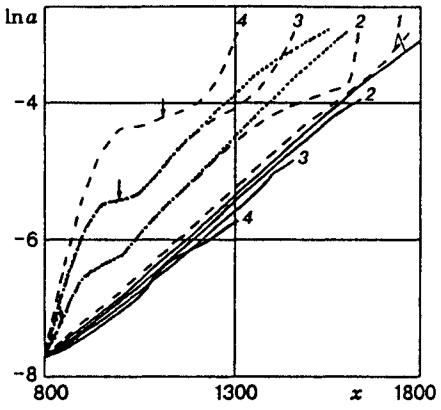

Fig. 2

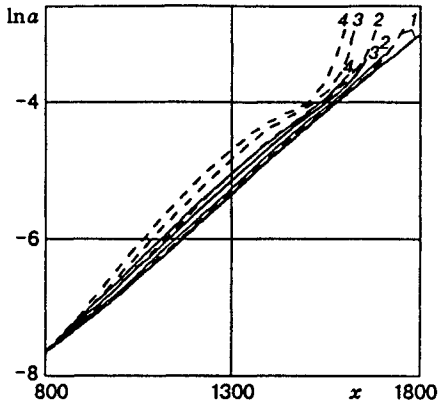

Fig. 3

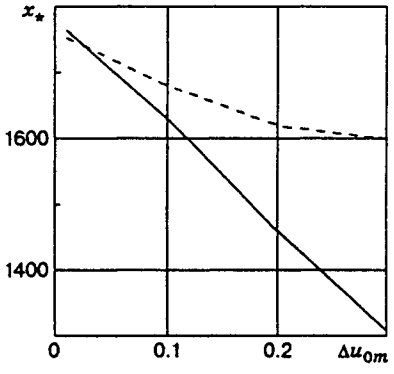

Fig. 4

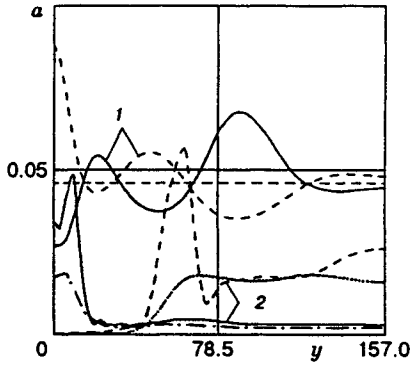

Fig. 5

curves in Figs. 2 and 3 correspond to the maximum amplitudes $a_m = \max_y a(y, z_0)$ with respect to y, and the solid curves correspond to the amplitudes of pulsations in the free stream in the middle between velocity defect regions. Curves 1–4 in Fig. 2 correspond to $\Delta u_{0m} = -0.01$, -0.1, -0.2, and -0.3, and curves 1–4 in Fig. 3 refer to $\Delta u_{0m} = 0.01$, 0.1, 0.2, and 0.3. The location of the transition versus $|\Delta u_{0m}|$ for negative and positive velocity defects is shown by the solid and dashed curves in Fig. 4.

It is seen from a comparison of Figs. 2 and 3 that, for small velocity defects (± 0.01), the sign of the velocity defect does not exert a substantial effect on the evolution of disturbances. In this case, at the linear stage of transition the maximum amplitude with respect to y differs slightly from its free-stream value, i.e., the inhomogeneity does not exert a substantial effect on the Tollmien–Schlichting wave evolution. The growth of pulsations at the maximum with respect to y begins to lead their growth in the free stream only at the nonlinear stage of transition, when the pulsation amplitude becomes of the order of 1%.

For $\Delta u_{0m} = \pm 0.01$, the distributions of the amplitude of pulsations with respect to y in cross sections located immediately before the transition are presented by curves 1 (dashed and solid) in Fig. 5; the functions $a(y)$ for the positive (dashed curve) and negative (solid curve) velocity defects are almost symmetric about the dashed straight line $a = 0.046$. This means that the three-dimensional portion of the pulsations develops almost linearly up to the very moment of transition and probably consists of secondary disturbances that grow on the background of the nearly plane Tollmien–Schlichting wave. This assumption confirms the qualitative agreement of the distributions of the pulsation amplitude with respect to y for $\Delta u_{0m} = \pm 0.01$ with the transverse distribution of the amplitude of secondary disturbances (generated by the interaction between an

instability wave and a point roughness) that was obtained analytically by the author [10]:

$$a(y) = Ae^{-Cy^2}[\cos\beta_* y + B(y/x)\sin\beta_* y + O(y/x)^2], \quad y/x \ll 1.$$

Here A, B, and C are constants, x is the distance from the roughness, and β_* is the transverse wave number corresponding to the most rapidly growing secondary disturbances. Calculations according to the theory of secondary instability [11] showed that β_* changes from 0.15 to 0.25 as the amplitude of the Tollmien–Schlichting wave increases from 0.01 to 0.05. An estimate of β_* on the basis of the width of the central maximum of the function $a(y)$ for $\Delta u_{0m} = 0.01$ yields 0.17, which lies within the range predicted by the theory of secondary instability. For velocity defects of ± 0.1 or more, the pictures of disturbance development with positive and negative velocity defects are appreciably different. For positive defects, the dependences of the functions a_m on x do not experience substantial changes as the velocity defect increases to 0.3. An increase in the velocity defect leads only to a slightly earlier (in comparison with the case $\Delta u_{0m} = 0.01$) beginning of the advancing growth of the maximum amplitude. The upstream shift of the transition point with growth of the velocity defect is comparatively small, compared with the case of a negative velocity defect (see Fig. 4). The weak destabilizing effect of the high-velocity stream is related to the effect of displacement of the unstable disturbances from the inhomogeneity region. This effect is demonstrated by the dependence $a(y)$ for $\Delta u_{0m} = 0.3$ that was obtained in the cross section $x = 1500$ before the beginning of the nonlinear stage of transition (the dashed curve in Fig. 5). Because of the small amplitude of pulsations in the inhomogeneity region, the nonlinear growth of disturbances begins whenever the level of pulsations is practically the same as in the free stream. Therefore, the presence of a region with a positive velocity defect does not lead to earlier attainment of the threshold amplitude of pulsations that is necessary for initiation of nonlinear processes and, hence, shifts the location of the transition only slightly.

For negative velocity defects ($\Delta u_{0m} \leqslant -0.1$), advanced growth of the maximum amplitudes with respect to y, compared with the free-stream pulsations, is observed from the very beginning. Then the growth rate of pulsation maxima decreases to the growth rate of the Tollmien–Schlichting wave in an undisturbed flow. Finally, when the transverse-maximum amplitude reaches the threshold value, nonlinear processes begin, which again lead to advanced growth of a_m.

The comparatively rapid growth of a_m in the beginning of the disturbance evolution can easily be explained by the inflection-type instability of the velocity profile in the inhomogeneity region. However, the growth rate of the maximum disturbances decreases drastically much before the point of velocity inflection at the center of the inhomogeneity disappears. Moreover, no noticeable change in the behavior of the function a_m versus x is observed at the sites where the inflection points disappear (they are shown by arrows in Fig. 2 for each value of Δu_{0m}). Therefore, the hypothesis that the initial growth of pulsation maxima is caused by the process of transition and, in a steady state, the value of a_m is proportional to the free-stream amplitude of the Tollmien–Schlichting wave seems more realistic. This is more clearly demonstrated by the curves of a_m versus x obtained in the linear approximation for $\Delta u_{0m} = 0.1$ and 0.2 (dashed curves 2 and 3 in Fig. 2), which are, on a long section, almost parallel to curve 1 corresponding to the plane instability wave in the free stream. This character of evolution of disturbances allows us to conclude that the mechanism of inflection-type instability is not realized in a narrow zone of flow inhomogeneity. A similar effect was observed in experiments on the evolution of artificially generated disturbances in a boundary layer with a transversely periodic inhomogeneity of the velocity profile [4, 5]. Despite the presence of an inflected profile during a major part of a period, the growth rate of disturbances with frequencies of the Tollmien–Schlichting waves did not exceed the growth rate of similar disturbances in a uniform boundary layer.

This phenomenon is apparently explained by the fact that disturbances that are amplified in a narrow zone should "fit" in it and, hence, should consist of a packet of oblique waves with large transverse wave numbers. An analysis of the stability of a transversely uniform flow with a velocity profile corresponding to the middle of the inhomogeneity region showed that, for sufficiently large β, all modes become decaying. The rapid growth of high-frequency pulsations observed in [5] is probably associated with the inflection-type character of the transverse velocity distribution. The longitudinal wavelength of these disturbances is comparatively small, and the transverse modulation does not prevent their growth.

The distribution of the pulsation amplitude relative to y at the end of the linear stage of transition ($x = 1200$) for $\Delta u_{0m} = -0.3$ is shown by the dot-and-dashed curve in Fig. 5. It is of interest that the maximum pulsations are not located in the center of the inhomogeneity region, but are shifted to its boundaries. A similar character of the transverse amplitude distribution (in measurements at a distance from the wall that corresponds to the maximum velocity defect) was observed in [5] for high-frequency disturbances. For a frequency corresponding to the Tollmien–Schlichting wave, similar distributions were measured in [4, 5] closer to the wall at the height of maximum pulsations. On the other hand, the maxima of the pulsation amplitude in these distributions corresponded to the maxima of the steady velocity component.

The most probable reason for the concentration of disturbances in the low-velocity stream and their displacement from the high-velocity stream that were observed in computations is the transverse inhomogeneity of the phase velocity of unstable disturbances. The phase velocity of the Tollmien–Schlichting wave is larger than in an undisturbed flow in the zone of a negative velocity defect and smaller in the zone of a positive velocity defect. According to the laws of geometrical optics, beams are concentrated in regions with a low phase velocity and are displaced from regions with a high velocity of propagating disturbances. The violation of this rule for low-frequency disturbances in [4, 5] can be explained by the fact that the period of inhomogeneity in these experiments is comparable with the instability wavelength and, therefore, the approximation of geometrical optics is no longer valid.

At the nonlinear stage of transition, for finite velocity defects the transverse distribution of velocity fluctuations is apparently determined by the shape of the packet of secondary disturbances developed on the background of the primary instability wave, which is strongly transversely nonuniform. Analysis of the processes that occur is substantially complicated by difficulties in dividing the total field of pulsations into the primary wave and secondary disturbances. Some qualitative features, however, can be deduced from a comparison of the functions $a(y)$ for $\Delta u_{0m} = -0.3$ and 0.3 immediately ahead of the transition (solid and dashed curves 2 in Fig. 5) with similar functions at the end of the linear stage of disturbance development (dot-and-dashed and dashed curves in Fig. 5). For example, at the nonlinear stage the pulsation maxima are shifted toward regions with larger gradients of the primary-wave amplitude. This shift can be explained by effective generation of three-dimensional secondary disturbances on the strong transverse inhomogeneity of the amplitude of pulsations of the primary wave.

It should be noted that because of the significant amplification of pulsations in the low-velocity region, nonlinear phenomena there begin at a very low free-stream amplitude of the instability wave. For example, for $\Delta u_{0m} = -0.3$ the nonlinear stage of transition at the center appears with a 0.25% amplitude of the Tollmien–Schlichting wave at the periphery. This effect can be the reason for the effect of a Tollmien–Schlichting wave with an amplitude of 0.1–0.2% on the transition process that was observed in [12] under conditions of high free-stream turbulence.

This work was supported by the International Science and Technology Center (Grant No. 199-95) and by the Russian Foundation for Fundamental Research (Grant No. 95-01-01201a).

REFERENCES

1. K. M. Butler and B. F. Farrell, "Three-dimensional optimal perturbations in viscous shear flows," *Phys. Fluids, A*, **4**, 1637–1650 (1992).
2. X. Yu and J. T. C. Lin, "The secondary instability in Görtler flow," *Phys. Fluids, A*, **3**, 1845–1847 (1991).
3. T. M. Fisher, S. Hein, and U. Dallmann, "A theoretical approach for describing the secondary instability features in the three-dimensional boundary layer flows," AIAA Paper No. 93-0080 (1993).
4. Y. S. Kachanov and O. I. Tararykin, "An experimental study of the stability of a relaxing boundary layer," *Izv. Sib. Otd. Akad. Nauk SSSR, Ser. Tekh. Nauk*, No. 18, 9–19 (1987).
5. A. A. Bakchinov, G. R. Grek, G. B. Klingmann, and V. V. Kozlov, "Transition experiments in a boundary layer with embedded streamwise vortices," *Phys. Fluids*, **7**, No. 4, 820–832 (1995).

6. F. P. Bertolotti, T. Herbert, and P. R. Spalart, "Linear and nonlinear stability of the Blasius boundary layer," *J. Fluid Mech.*, **242**, 441–474 (1992).
7. S. V. Manuilovich, "On receptivity of a subsonic flow to oscillatory actions localized on the bottom of a boundary layer," *Izv. Akad. Nauk SSSR, Mekh. Zhidk. Gaza*, No. 4, 63–69 (1988).
8. T. Herbert, "Boundary-layer transition — analysis and prediction revised," AIAA Paper No. 91-0737 (1991).
9. K. J. A. Westin, A. V. Boiko, G. B. Klingmann, et al., "Experiments in a boundary layer subjected to free-stream turbulence. Pt. 1. Boundary layer structure and receptivity," *J. Fluid Mech.*, **281**, 193–218 (1994).
10. M. V. Ustinov, "Generation of secondary instability modes upon interaction of a Tollmien–Schlichting wave with roughness," *Izv. Ross. Akad. Nauk, Mekh. Zhidk. Gaza*, No. 3, 28–38 (1995).
11. T. Herbert, F. P. Bertolotti, and G. R. Santos, "Floquet analysis of secondary instability in shear flows," in: D. L. Dwoyer and M. Y. Hussaini (eds.), *Stability of Time-Dependent and Spatially Varying Flows*, Springer, New York (1987), pp. 43–57.
12. A. V. Boiko, K. J. A. Westin, B. G. B. Klingmann, et al., "Experiments in a boundary layer subjected to free-stream turbulence. Pt. 2. The role of T–S waves in the transition process," *J. Fluid Mech.*, **281**, 219–245 (1994).